Structural properties of magnesium and aluminium co-substituted lithium ferrite

ARTICLE *in* MATERIALS LETTERS · AUGUST 2003

Impact Factor: 2.27 · DOI: 10.1016/S0167-577X(03)00263-5

6 AUTHORS, INCLUDING:

Kunal Modi
Saurashtra University
73 PUBLICATIONS **453** CITATIONS
SEE PROFILE

M. C. Chhantbar
Shankersinh Vaghela Bapu Institute of…
20 PUBLICATIONS **118** CITATIONS
SEE PROFILE

Available online at www.sciencedirect.com
SCIENCE DIRECT®
ELSEVIER
Materials Letters 57 (2003) 4049–4053
MATERIALS LETTERS
www.elsevier.com/locate/matlet

Structural properties of magnesium and aluminium co-substituted lithium ferrite

K.B. Modi*, J.D. Gajera, M.C. Chhantbar, K.G. Saija, G.J. Baldha, H.H. Joshi

Department of Physics, Saurashtra University, Rajkot 360 005, India

Received 18 July 2002; received in revised form 11 November 2002; accepted 25 February 2003

Abstract

The structural properties of Mg^{2+} and Al^{3+} co-substituted $Li_{0.5}Fe_{2.5}O_4$ are studied by synthesizing the spinel solid solution series $Mg_xAl_{2x}Li_{0.5(1-x)}Fe_{2.5(1-x)}O_4$. Polycrystalline samples of this series with $x = 0.0$, 0.1, 0.2, 0.3, 0.4 and 0.5 have been prepared by double-sintering ceramic method. The structural details like: lattice constant and distribution of cations in the tetrahedral and octahedral interstitial voids have been deduced through X-ray diffraction (XRD) data analysis. The x dependence of bond length, oxygen positional parameter, site ionic radii, bulk density, porosity and shrinkages have also been determined.

Keywords: Ferrites; Structural properties; Cation distribution; Inter-ionic distances

1. Introduction

Ferrites possess high values of magnetization because of imbalanced site magnetic moments along with high values of resistivity, low dielectric loss and high Neel temperatures. These properties have made them versatile materials for various technological applications. The crystallographic, electrical and magnetic properties of ferrites depend strongly upon stoichiometry as well as processing parameters such as temperature, atmosphere and pressure, which affect the distribution of cations among the available tetrahedral (A) and octahedral (B) sites in the spinel lattice. Control over cation distribution and the oxygen parameter provide a means of developing the desired physical properties for their proper use in industry.

For more than a decade, lithium ferrite materials have dominated in the field of microwave applications. Lithium ferrite with suitable substitutes is a well-known promising candidate for high frequency applications. Several series of compositions of lithium ferrite covering a wide range of properties have become available commercially.

There are many reports in the literature on the effect of non-magnetic and magnetic cation substitution on various properties of lithium ferrite [1–4]. Recently, we have reported structural and magnetic properties of Al and Cr co-substituted lithium ferrite by means of X-ray diffraction (XRD), magnetization, a.c. susceptibility and Mossbauer spectroscopy measurements [5]. The structural parameters like lattice constant, cation distribution, X-ray density, particle size, oxygen position parameters, of Cd- and Al-substituted cobalt ferrite was studied by Jadhav et al. [6], while such parameters were studied by Riet-

* Corresponding author.
E-mail address: kunalbmodi2003@yahoo.com (K.B. Modi).

0167-577X/03/$ - see front matter © 2003 Elsevier Science B.V. All rights reserved.
doi:10.1016/S0167-577X(03)00263-5

veld refinement of X-ray diffraction patterns of Gd substituted Mn–Zn ferrite magnetic fluids by Upadhyay and Parekh [7] and of Mn–Cr ferrite by higher angle neutron diffraction data by Zakaria et al. [8].

Recently, the bulk magnetic properties of Mg^{2+} and Al^{3+} co-substituted $Li_{0.5}Fe_{2.5}O_4$ with generic formula $Mg_xAl_{2x}Li_{0.5(1-x)}Fe_{2.5(1-x)}O_4$ [9] have been reported. No systematic study of cation distribution and concentration dependence of structural parameters such as lattice constant, X-ray density, porosity, shrinkages, ionic radii, bond length, etc. has been reported on the present system. In the present communication, the effect of co-substitution of magnesium and aluminium on some structural properties of lithium ferrite with the generic formula $Mg_xAl_{2x}Li_{0.5(1-x)}Fe_{2.5(1-x)}O_4$ ($x=0.0$, 0.1, 0.2, 0.3, 0.4 and 0.5) are reported with the aim of developing sintered material with properties that can be tailored to the requirements of the device engineers.

2. Experimental details

Six samples of Mg^{2+} and Al^{3+} co-substituted $Li_{0.5}Fe_{2.5}O_4$ with the generic formula $Mg_xAL_{2x}Li_{0.5(1-x)}Fe_{2.5(1-x)}O_4$ ($x=0.0$, 0.1, 0.2, 0.3, 0.4 and 0.5) were prepared by usual double sintering ceramic technique. The starting materials were MgO, Al_2O_3, Li_2CO_3 and Fe_2O_3, all 99.3% pure and supplied by E. Merck. The oxides were mixed thoroughly in stoichiometric proportion to yield the desired composition and wet ground. The mixture was dried and pressed into pellets. These pellets were calcined at 950 °C for 24 h. In final sintering process, samples were kept at 1150 °C for 24 h and slowly cooled to room temperature at the rate of 2 °C/min. The X-ray diffraction patterns for all the compositions were recorded at 300 K with a Philips (PM 9220) diffractometer using FeK_α radiation.

3. Results and discussion

The room temperature (300 K) X-ray diffraction patterns of each composition corresponded to well defined crystalline fcc phase and confirmed the spinel structure. The concentration dependence of lattice constant a with an accuracy of ± 0.002 Å determined from XRD data for $x=0.0$–0.5 is shown in Fig. 1(a).

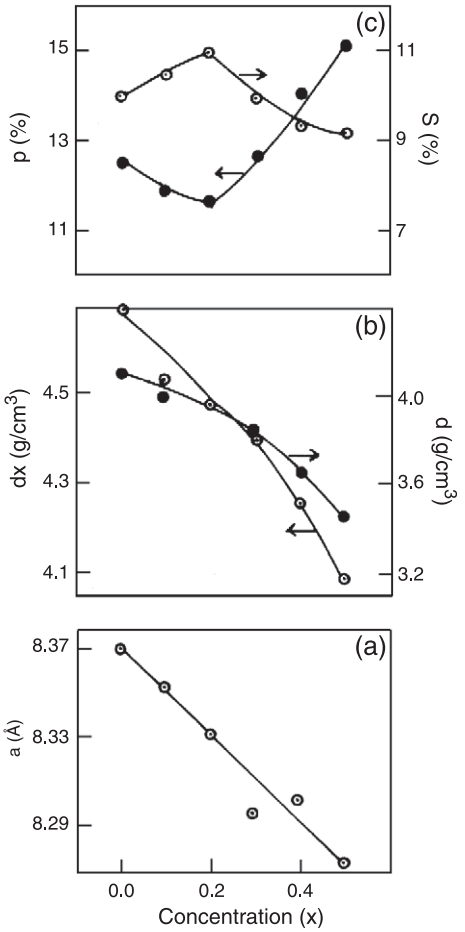

Fig. 1. Variation of (a) lattice constant, (b) X-ray density and bulk density, (c) porosity and shrinkages with concentration (x).

The lattice constant gradually decreases with increasing x, obeying the Vegard's law [10]. Usually, in a solid solution of spinels within the miscibility range, a linear change in the lattice constant with the concentration of the components is observed [10]. The linear decrease in the lattice constant is due to the replacement of larger Li^{1+} (0.70 Å) and Fe^{3+} (0.64 Å) ions by smaller Al^{3+} ions with an ionic radius of 0.51 Å.

In order to determine the cation distribution, X-ray intensity calculations were made using formula suggested by Buerger [11]:

$$I_{hkl} = |F_{hkl}|^2 \cdot P \cdot L_p$$

where, I_{hkl} is the relative integrated intensity, F_{hkl} is the structure factor, P is the multiplicity factor and L_p is the Lorentz polarization factor $=(1+\cos^2\theta/\sin^2\theta\cdot\cos^2\theta)$.

According to Ohnishi and Teranishi [12], the intensity ratios of planes I(220)/I(400) and I(400)/I(422) are considered to be sensitive to the cation distribution parameters (x). The ionic configuration based on site preference energy values proposed by Miller [13] for individual cations in $Mg_xAl_{2x}Li_{0.5(1-x)}Fe_{2.5(1-x)}O_4$ suggests that Li^{1+} and Al^{3+} occupy only B-sites where as Mg^{2+} and Fe^{3+} ions occupy A- and B-sites. There is a good contrast in the atomic scattering factors of Fe^{3+} and the other cations present in the system. This makes the determination of cation distribution quite reliable. Moreover, any alteration in the distribution of cations causes significant change in the theoretical values of X-ray diffraction intensity ratios. Therefore, in the process of arriving at the final cation distribution, the site occupancy of all the cations was varied for many combinations and the typical illustrations are shown in Table 1. The final cation distributions were deduced by simultaneously considering the Bragg plane ratios, the fitting of the magnetization data at 80 K and theoretical determination of lattice constant values. It is evident from Table 1 that Li^{1+} and Al^{3+} ions occupy only B-sites, while Mg^{2+} and Fe^{3+} ions occupy both the sites.

It is worthwhile to note that about 80% Mg^{2+} ion occupy A-sites, while occupation of Fe^{3+} on B-site ranges from 50% to 60% within the range studied. The study has revealed the B-site preference of Li^{1+}, Mg^{2+}, Al^{3+} and Fe^{3+} as follows: $Li^{1+} \approx Al^{3+} > Fe^{3+} > Mg^{2+}$. Besides using experimentally found values of lattice constant and oxygen parameters (u) [14], it is possible to calculate the value of the mean ionic radius per molecule of the tetrahedral and octahedral sites, r_A and r_B, respectively, using the cation distribution for each composition using the relations [15]:

$$r_A = C_{AMg}r(Mg^{2+}) + C_{AFe}r(Fe^{3+})$$

$$r_B = \frac{1}{2}[C_{BMg}r(Mg^{2+}) + C_{BFe}r(Fe^{3+}) + C_{BLi}r(Li^{1+}) + C_{BAl}r(Al^{3+})]$$

where $r(Li^{1+})$, $r(Mg^{2+})$, $r(Al^{3+})$ and $r(Fe^{3+})$ are ionic radii of Li^{1+}, Mg^{2+}, Al^{3+} and Fe^{3+} ions, respectively, while C_{AMg} and C_{AFe} are the concentrations of the Mg^{2+} and Fe^{3+} ions on A-sites and C_{BMg}, C_{BFe}, C_{BLi} and C_{BAl} are concentrations of Mg^{2+}, Fe^{3+}, Li^{1+} and Al^{3+} ions on B-sites.

Using these formulae, the values of mean tetrahedral and octahedral ionic radii for each composition have been calculated and are listed in Table 2. It can be seen that mean tetrahedral ionic radius increases

Table 1
Comparison of X-ray intensity ratios for estimating cation distribution

x	A-site	B-site	I(220)/I(400)		I(400)/I(422)	
			Obs.	Cal.	Obs.	Cal.
0.0	$Fe_{1.0}$	$Li_{0.5}Fe_{1.5}$	1.50	1.51	1.93	1.99
0.1	$Li_{0.09}Fe_{0.91}$	$Li_{0.36}Al_{0.36}Mg_{0.1}Fe_{1.34}$		1.17		1.72
	$Mg_{0.09}Fe_{0.91}$	$Li_{0.45}Al_{0.2}Mg_{0.01}Fe_{1.34}$	2.35	2.05	1.87	1.48
	$Li_{0.045}Al_{0.02}Mg_{0.025}Fe_{0.91}$	$Li_{0.405}Al_{0.18}Mg_{0.075}Fe_{1.34}$		1.91		1.60
0.2	$Li_{0.08}Mg_{0.08}Fe_{0.84}$	$Li_{0.32}Al_{0.4}Mg_{0.12}Fe_{1.16}$		1.73		1.76
	$Mg_{0.16}Fe_{0.84}$	$Li_{0.4}Al_{0.4}Mg_{0.04}Fe_{1.16}$	2.02	1.97	1.99	1.54
	$Li_{0.04}Al_{0.04}Mg_{0.08}Fe_{0.84}$	$Li_{0.36}Al_{0.36}Mg_{0.12}Fe_{1.16}$		1.85		1.64
0.3	$Li_{0.07}Mg_{0.17}Fe_{0.76}$	$Li_{0.28}Al_{0.6}Mg_{0.13}Fe_{0.99}$		1.64		1.85
	$Mg_{0.24}Fe_{0.76}$	$Li_{0.35}Al_{0.6}Mg_{0.06}Fe_{0.99}$	2.17	1.85	1.53	1.64
	$Li_{0.035}Al_{0.06}Mg_{0.145}Fe_{0.76}$	$Li_{0.315}Al_{0.54}Mg_{0.155}Fe_{0.99}$		1.75		1.73
0.4	$Li_{0.06}Mg_{0.26}Fe_{0.68}$	$Li_{0.24}Al_{0.8}Mg_{0.14}Fe_{0.82}$		1.56		1.94
	$Mg_{0.32}Fe_{0.68}$	$Li_{0.3}Al_{0.8}Mg_{0.08}Fe_{0.82}$	2.21	1.73	1.51	1.74
	$Li_{0.03}Al_{0.08}Mg_{0.21}Fe_{0.68}$	$Li_{0.27}Al_{0.72}Mg_{0.19}Fe_{0.82}$		1.65		1.82
0.5	$Li_{0.05}Mg_{0.37}Fe_{0.58}$	$Li_{0.2}Al_{1.0}Mg_{0.13}Fe_{0.67}$		1.38		2.19
	$Mg_{0.42}Fe_{0.58}$	$Li_{0.25}Al_{1.0}Mg_{0.08}Fe_{0.67}$	1.92	1.51	1.99	1.99
	$Li_{0.025}Al_{0.1}Mg_{0.295}Fe_{0.58}$	$Li_{0.225}Al_{0.9}Mg_{0.205}Fe_{0.67}$		1.45		2.05

Table 2
Lattice constant (a), ionic radii (r) and oxygen positional parameter (u) for Mg–Al–Li–Fe–O system

Concentration (x)	a_{exp} (Å) ± 0.002 Å	a_{th} (Å)	r_A (Å)	r_B (Å) ± 0.002 Å	$\bar{r}$ (Å)	u (Å)
0.0	8.370	8.368	0.040	0.655	0.647	0.2600
0.1	8.353	8.346	0.650	0.641	0.645	0.2602
0.2	8.332	8.324	0.658	0.628	0.643	0.2604
0.3	8.298	8.302	0.666	0.615	0.641	0.2606
0.4	8.303	8.290	0.675	0.606	0.640	0.2608
0.5	8.275	8.258	0.686	0.587	0.636	0.2610

continuously with increasing (x). It is observed that ionic radius of octahedral site decreases with increasing (x) which in turn causes the lattice constant a, to decrease with x. The decrease in r_B suggests the replacement of larger Li^{1+} and Fe^{3+} ions by smaller Al^{3+} ions on the B-site (Table 1). As such, it can be concluded that the octahedral site substitution plays a dominant role in influencing the value of the lattice constant. A similar result has been found in our earlier work on $MgAl_xFe_{2-x}O_4$ system [16] Moreover, it is found that the average ionic radius $\bar{r} = ((r_A + r_B)/2)$ decreases slowly with increasing concentration (x), which is reflected in a decrease in a with x (Table 2).

It is known that there is a correlation between the ionic radius and the lattice constant. The lattice constant can be calculated theoretically by the relation suggested by Mazen et al. [17]:

$$a_{th} = \frac{8}{3\sqrt{3}}[(r_A + R_0) + \sqrt{3}(r_B + R_0)]$$

where R_0 is the radius of the oxygen ions (1.32 Å). The agreement between a_{th} and a_{exp} obtained from X-ray data indirectly supports the cation distribution deduced from X-ray intensity calculations. The theoretical values of the lattice constant (a_{th}) as a function of concentration (x) are shown in Table 2. It is seen that there is reasonable agreement between experimentally and theoretically found values of lattice constant suggesting that the estimated cation distribution is in agreement with real distribution in that range. It is seen from Table 2 that the experimental error (the difference between a_{th} (Å) and a_{exp} (Å)) increases with increasing x. The increase in the difference with x indicates the possibility of the effects like "covalency", which could not be considered in the theoretical model.

The variation of bulk density (d) as well as the X-ray density (d_x) with chemical composition (x) is shown in Fig. 1(b). In order to determine the bulk density of a specimen in pellet form, the precise values of weight measured through electronic balance and the volume measured by using traveling microscope were used. The X-ray density for each composition was calculated using the relation [18]:

$$d_x = ZM/Na^3$$

where Z is the number of molecules per unit cell ($Z = 8$) of spinel lattice, M the molecular weight of the ferrite sample, N is Avogadro's number and a the lattice constant of the ferrite.

The X-ray density and bulk density decrease with increase of x, i.e. the bulk density reflects the same general behaviour of the theoretical density (Fig. 1(b)). This can be ascribed to the atomic weight and density of Mg^{2+} (24.31 and 1.74 g/ml) and Al^{3+} (26.98 and 2.70 g/ml), which are lower than those of Fe^{3+} (55.8 and 7.87 g/ml).

The percentage porosity (P) was calculated using the relation [18]:

$$P = (1 - d/d_x) \times 100\%$$

The change of P and percentage shrinkage of the diameter of the disc shape samples before and after final sintering process, with composition is shown in Fig. 1(c). As expected porosity and shrinkage behave inversely to each other with respect to concentration (x). The variation of porosity (P) with x depends upon the relative values of X-ray density (d_x) and the bulk density (d) and the trend of P versus x depicted in Fig. 1(c) is the result of the interplay of d_x and d.

The configurations of ion pairs in spinel ferrites with favourable distances and angles for effective magnetic interaction are shown in Fig. 2. The bond lengths between the cations (b, c, d, e and f) (Me–Me) and between the cation and anion (p, q, r and s) (Me–

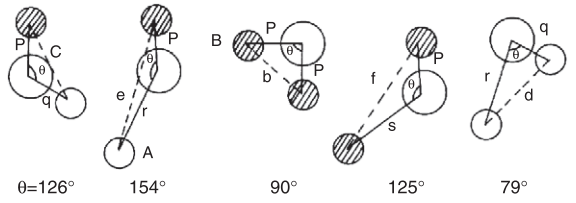

Fig. 2. Configuration of the ion pairs in spinel ferrites with favourable distances and angles for effective magnetic interactions.

Table 3
Bondlengths between cation–anion (Me–O) and cation–cation (Me–Me)

Concentration (x)	Me–O (Å)				Me–Me (Å)				
	p	q	r	s	b	c	d	e	f
0.0	2.01	1.96	3.75	3.67	2.96	3.47	3.62	5.44	5.13
0.1	2.00	1.96	3.74	3.67	2.95	3.46	3.62	5.42	5.11
0.2	2.00	1.95	3.74	3.66	2.95	3.45	3.61	3.41	5.10
0.3	1.99	1.95	3.73	3.64	2.93	3.44	3.59	5.39	5.08
0.4	1.99	1.95	3.74	3.65	2.93	3.44	3.59	5.39	5.08
0.5	1.98	1.95	3.73	3.63	2.92	3.43	3.58	5.37	5.07

O) were calculated using the experimental values of lattice constant and oxygen positional parameter (u) by the relations [19,20]:

Me–O	Me–Me
$p = a(1/2 - u)$	$b = (a/4)2^{1/2}$
$q = a(u - 1/8)3^{1/2}$	$c = (a/8)11^{1/2}$
$r = a(u - 1/8)11^{1/2}$	$d = (a/4)3^{1/2}$
$s = a/3(u + 1/2)3^{1/2}$	$e = (3a/8)3^{1/2}$
	$f = (a/4)6^{1/2}$

The oxygen positional parameter (u) for each composition were deduced from the value of u for two end members $Li_{0.5}Fe_{2.5}O_4$ ($x = 0.0$) ($u = 0.260$ Å) and $MgAl_2O_4$ ($x = 1.0$) ($u = 0.262$ Å) obtained from the literature [14,21] and tabulated in Table 2.

From the Table 3, it is seen that both bond lengths between Me–O and Me–Me decreases with increasing concentration (x). The decreases in Me–O and Me–Me bond lengths with x may be due to substitution of Mg^{2+} ions with larger ionic radius on both the site replaces the Fe^{3+} and Li^{1+} with smaller ionic radius, which decrease the Me–O and Me–Me distances.

The decrease in Me–O and Me–Me distances should result in the enhancement of strength of magnetic interactions but the replacement of magnetic Fe^{3+} by non-magnetic Mg^{2+} and Al^{3+} reduces the strength of magnetic interactions in the system.

4. Conclusions

The simultaneous substitution for Li^{1+} and Fe^{3+} by Mg^{2+} and Al^{3+} in $Li_{0.5}Fe_{2.5}O_4$ has revealed the B-site preference of cations involved as: $Li^{1+} \approx Al^{3+} > Fe^{3+} > Mg^{2+}$. The distribution of cations in the interstitial sites determined through X-ray diffraction has been confirmed by theoretical calculations of lattice constant values. The bond lengths can be calculated theoretically. It is interesting to note that the compositional variation of magneton number and Neel temperature can be understood in light of structural parameters. Therefore, it is important to consider the effect of structural parameters on transport properties while synthesizing the ferrite materials for specific applications.

Acknowledgements

One of the authors (KBM) is thankful to the Department of Science and Technology, New Delhi for providing financial assistance under Young Scientist Research Project Scheme (HR/SY/P-03.97).

References

[1] S.S. Bellad, R.B. Panja, Mater. Chem. Phys. 52 (1998) 166.
[2] U.N. Trivedi, K.H. Jani, K.B. Modi, H.H. Joshi, J. Mater. Sci. Lett. 19 (2000) 1271.
[3] D. Ravinder, Mater. Lett. 40 (1999) 205.
[4] D. Ravinder, Mater. Lett. 40 (1999) 198.
[5] U.N. Trivedi, K.B. Modi, H.H. Joshi, PRAMANA 58 (2002) 1031.
[6] A.R. Shitre, U.N. Deratwal, D.S. Birajdar, K.M. Jadhav, Indian J. Eng. Mater. Sci. 7 (2000) 464.
[7] T. Upadhyay, K. Parekh, Indian J. Pure Appl. Phys. 40 (2002) 282.
[8] A.K.M. Zakaria, M.A. Asgar, F.U. Ahmed, A.K. Azad, S.M. Unas, S.K. Paranjpe, A. Das, Indian J. Pure Appl. Phys. 40 (2002) 46.
[9] G.J. Baldha, K.G. Saija, K.B. Modi, H.H. Joshi, R.G. Kulkarni, Mater. Lett. 53 (2002) 233.
[10] C.G. Whinfrey, D.W. Eckart, A. Tauber, J. Am. Chem. Soc. 82 (1960) 2695.
[11] M.J. Buerger, J. Crystal Structure Analysis, Wiley, NY, 1960.
[12] H. Ohnishi, T. Teranishi, J. Phys. Soc. Jpn. 16 (1961) 36.
[13] A. Miller, J. Appl. Phys. 30 (1959) 245.
[14] K.J. Standly, Oxide Magnetic Material, Clarendon Press, Oxford, 1972.
[15] A. Globus, H. Pascard, V. Cagan, J. Phys., Suppl. 438 (C-1) (1977) 439.
[16] K.B. Modi, H.H. Joshi, J. Mater. Sci. Lett. 17 (1998) 741.
[17] S.A. Mazen, M.H. Abdallah, B.A. Sabrah, H.A.M. Hasham, Phys. Status Solidi, A 134 (1992) 263.
[18] J. Smith, H.P.J. Wijn, Ferrites, Philips, Eindhoven, 1959.
[19] J.B. Goodenough, J. Phys. Chem. Solids 6 (1958) 287.
[20] J. Kanamori, J. Phys. Chem. Solids 10 (1959) 67.
[21] S.C. Watawe, PhD Thesis, Kolhapur University, Kolhapur, India, 2000.